A Master-Slave Operating Technique for Material Removal Processes

Arayavongkul R. and Sangveraphunsiri V.

Department of Mechanical Engineering, Faculty of Engineering, Chulalongkorn University, Bangkok, Thailand

Abstract

This paper presents a master-slave operating technique for the material removal process aimed to be used for part prototyping. This system is designed for 5-axis milling processes which consist of a 6-DOF parallel haptic device as a master arm and a hybrid 5-axis H4 family parallel manipulator as a slave. According to the dissimilar structures between the master and slave, an operating technique to define positions and orientations of the slave's end effecter or milling tool is applied in Cartesian space. Force reflection techniques in this work can help the operator move the master arm's handle firmly along the virtual wall and generate significant feeling of force in master-slave milling tasks. The results of ball-end milling tasks show that each reproduced wooden work piece is similar to its referenced object with an average error of about 1 mm on each side and this master-slave operating technique can be used for dimensional scaling tasks.

Keywords*: Master-Slave / Haptic / Parallel Manipulator/ Force Reflection*

1 Introduction

Milling is a common process of machining to remove materials from a stock. For building a complex geometry part, such as mold, die, automotive parts, aerospace component, etc., multiple-axis machine tools, such as a 5-axis CNC milling machines with ball-end tool, is typical used to produce complex surfaces [3,4]. The cutting conditions such as feed-rate, depth of cut, and spindle speed, used in the material removal processes, need to be carefully studied and selected. This will affect directly to the quality of surfaces obtained as well as productivity [9]. If the model of a required part exists, a CAD/CAM software with reverse engineering techniques can be used to reconstructed surfaces of the part. And cutting tool paths can be generated from the reconstructed surfaces by specifying necessary cutting processes in the CAM software. However, working with surface reconstruction may take a long time due to the part's complexity. And it may need special CAD/CAM features concerning the reversed engineering technique and complex surface reconstruction. Some researchers worked on the tool path generating procedure such as: [1] proposes a method to generate three-axis ball-end milling tool paths directly from discrete data point sets received from a scanning process and [2] investigates 5-axis tool paths generated from cloud points using 3D fitting scheme. The direct tool paths from an existing cloud point can reduce the time in the reverse engineering process, however the finishing surface quality depends on the engaged area between the milling tool and contact surfaces.

A master–slave manipulator can be applied on multi-purposed tasks such as extend the human reach to manipulate in hazardous locations, pick and place or a teleoperation-based robotic-assisted surgery with serial mechanisms [5,8]. In this work, the 5-axis milling machine based on H4-parallel configuration is developed and used as slave manipulator arm. Although a manipulator with parallel mechanism has small working volume, the benefits of this parallel mechanism such as structural stiffness, payload capacity and acceleration performance are still favored in many research activities. Thus, this paper proposes a master-slave operating technique applied to the parallel mechanisms for the material removal processes. The proposed master-slave operating system can generates tool-path from a referenced object with a master arm and removes the material from a stock with the slave arm, simultaneously. This technique will reduce the time spending for tool-path generating procedures, because the system

can generate milling tool-path directly from coordinate points captured by the master arm. Point intervals can be specified by a sampling period of the control system. The position error between the desired tool-tip position, from the master arm, and the actual tool-tip position, from the slave arm, is used for generating reflecting force at the master arm felt by an operator. The operator should receive a suitable force reflection against his hand while the milling machine is performing cutting processes to ensure the suitable cutting conditions are selected indirectly. The feeling of cutting forces appeared to the operator through the master arm can be adjusted by adjusting the parameters in the position-force control algorithm which will not be mentioned in this paper. It will be reported later by the researchers soon. In this paper, the controller, used for controlling motions of each axis of the 5-axis milling machine, is PD controller. The dynamics of linkages, for this H4 parallel configuration, are assumed small due to high transmission ratio and low speed motion.

2 The Master-Slave system

The master-slave operating system considered in this work is shown in Figure 1. As mention before, both manipulator arms are based on parallel configuration or mechanism. The master arm is used to generate the reference position and orientation for the slave arm controller. From the angles measured by nine encoders attached at some specific joints of the master arm, the end-point position and orientation can be obtained by a forward kinematic of the master arm, derived later. In this way, the operator moves the end-tip of the master arm along the desired surface area. The end-tip of the master arm is used to map to the end-tip position and orientation of the slave arm by a selected scale factor. The end-tip position and orientation of the slave arm are used to find the motion of each actuator of the slave arm by using inverse kinematic of the slave arm. Both the master arm and slave arm are moved simultaneously. The error between the end-tip position and orientation of the master arm and slave arm are used to generate force reflection at the master arm. The operator hand can feel this force reflection and can used this feeling to better control the motion of the cutting tool compared with no force reflection.

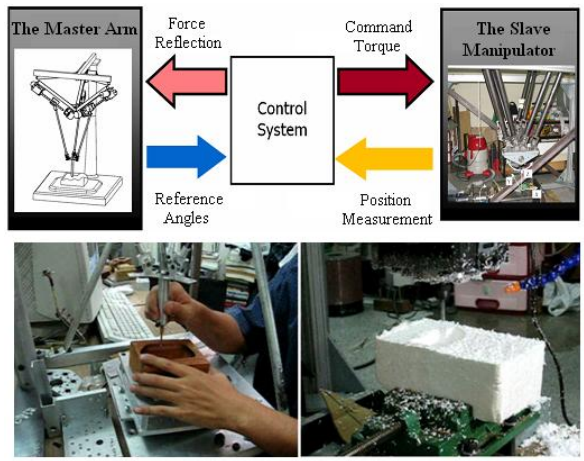

Figure 1: The master-slave system

The control system of the master-slave operation in this work is shown in the diagram in Figure 2. The master arm has three sub-linkage and each sub-linkage has three joints. So, there are totally nine joints attached with encoders. This angular information is used to calculate the tip position and orientation using forward kinematics. Then the controller will map this position and orientation of the master arm to the slave arm with a specified scale factor. This mapping position and orientation of the salve arm will be used to find the motion of each actuator of the slave arm by using inverse kinematics. Then, the PD control of the slave arm will control each servomotor, attached at each joint, to the desired position.

The actual position and orientation of the end-tip of the slave arm can be calculated from the forward kinematics of the slave arm by using the position information measured at each joint of the slave arm The actual position and orientation of the end-tip of the slave arm can be compared with the position and orientation obtained for the mapping to generate the position error and orientation error. These errors are used for generating force reflection needed to exert at the operator hand. In the force reflection loop, a virtual wall is added to limit the operator's movement into some specified restricted regions. This virtual wall is to help operator feel more comfortable when cutting position is closed to the boundary of the cutting volume.

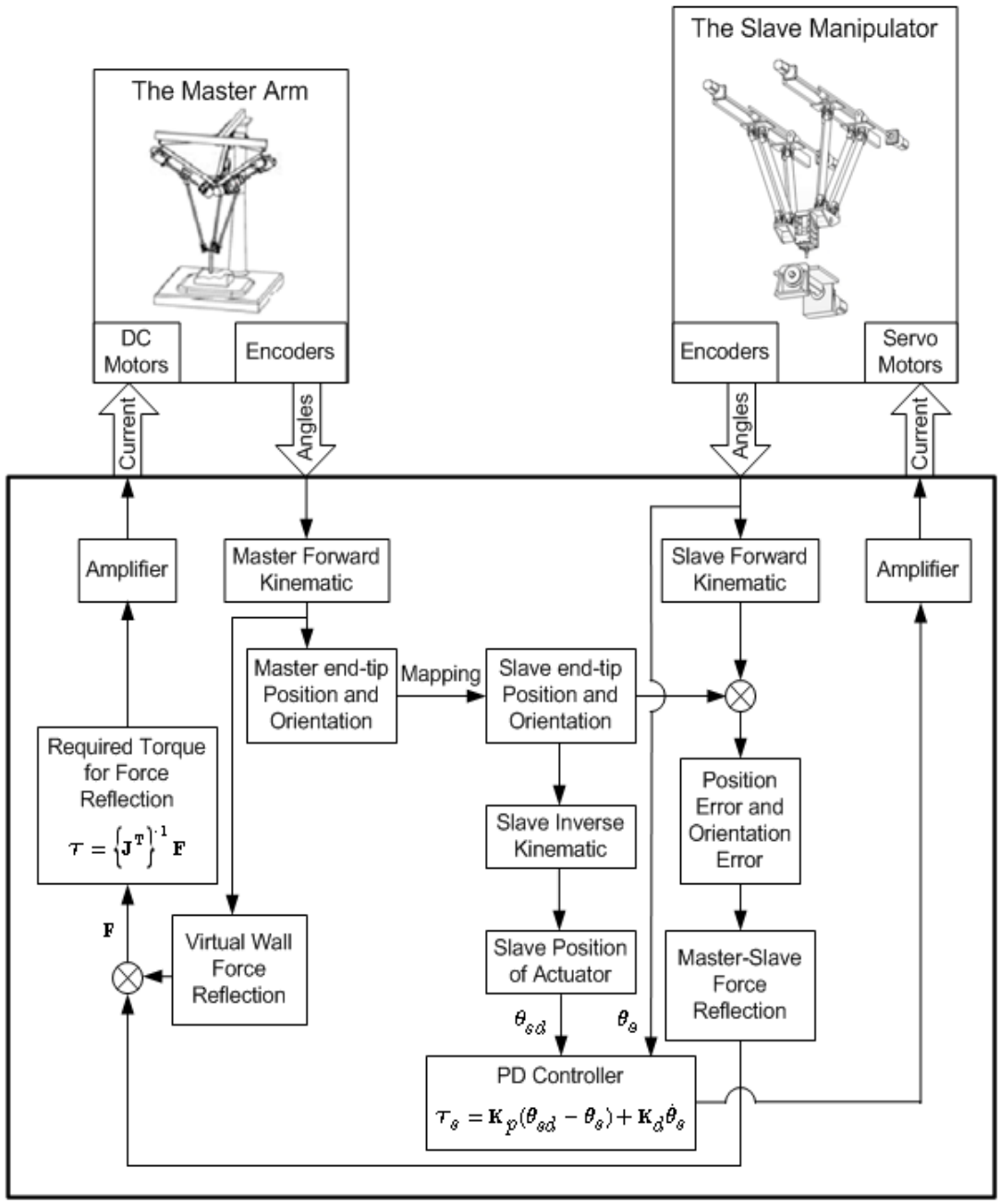

Figure 2: The control system's diagram

The master arm developed for this project has six degrees of freedom with a tendon-pulley driven mechanism as shown in Figure 3. The master arm has three sub-linkages of tendon-pulley system joining the base frame. DC motors are attached to the base frame for force reflection generating against the operator's hand.

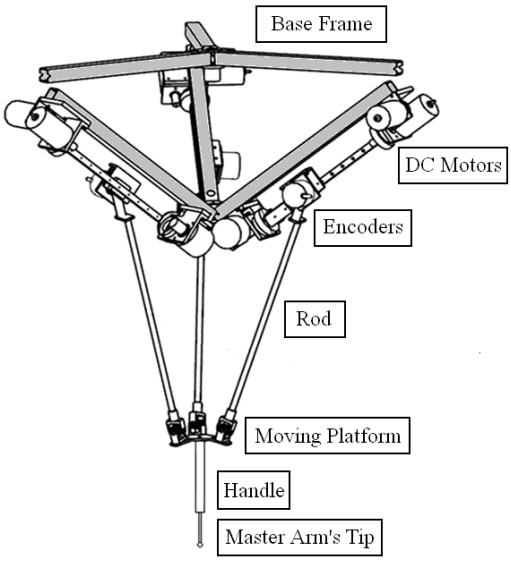

Figure 3: The master arm
(6-DOF parallel haptic device)

The slave manipulator shown in Figure 4 is a five-axis parallel manipulator in the H-4 family. The parallel configuration, which is actuated by a servo motor on each sliding joint or prismatic joint, has four degrees of freedom. This manipulator consists of three degrees of freedom on translation in X, Y, and Z directions and one degree of freedom in rotation about Y axis. The other degree of freedom is completed by a rotating table.

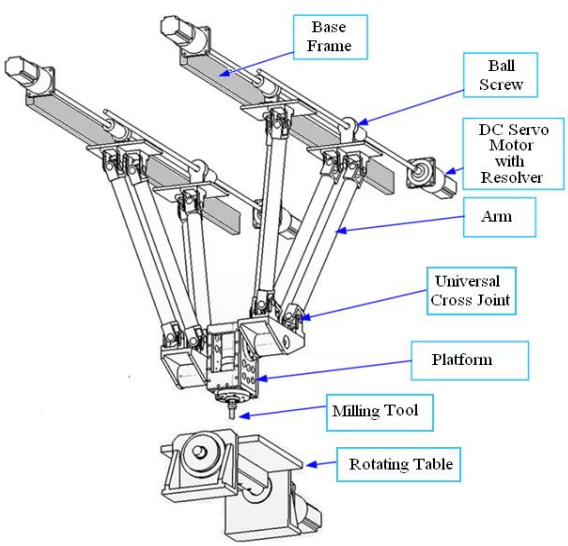

Figure 4: The components of the 5-axis H-4 family parallel manipulator

3 The Master-Slave Mathematical Model

3.1 *Forward kinematic of the master arm*

The forward kinematics of the master arm's tip can be derived starting from the base of the structure. As illustrated in Figure 5, the origin of the moving platform $\{M\}$ can be found with respect to the origin of the base frame $\{B\}$. The origin of coordinate frame1 is located at one end of the prismatic joint and frame 2 is attached to the center of the sliding joint which moves in the direction along the prismatic joint. The origins of frame 3 and frame 4 are located at the same position of the origin of frame 2. So, frame 2 is for sliding along the arm link, frame 3 is for rotating about the arm link, and frame 4 is for rotating about Z_4 which is perpendicular to Z_2 and Z_3. Frame 5 is attached to the universal joint at a corner of the moving platform.

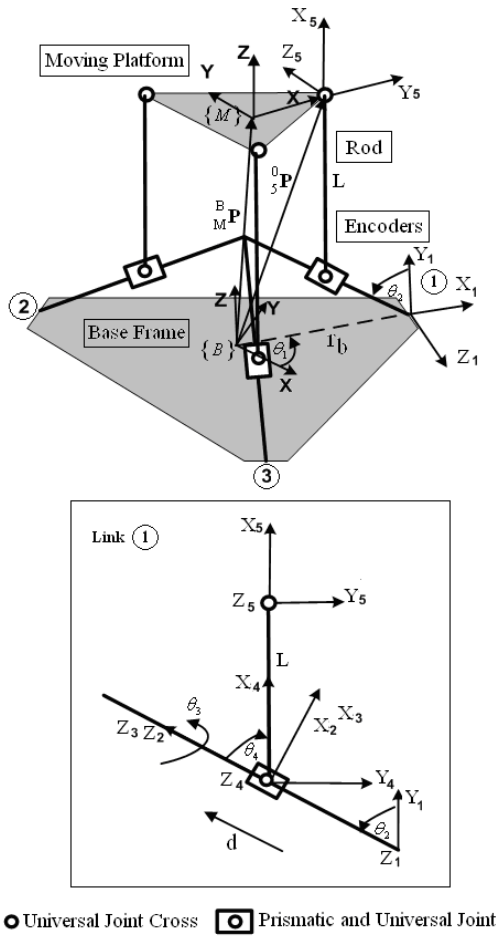

Figure 5: The unit-vector of each frame specified on each joint with respect to the base frame

The origin of coordinate frame5 belongs to link *i* which is respect to the base frame (*i* = 1, 2, 3) can be written in equation (1) :

$$\begin{bmatrix} {}^{B}_{5}\mathbf{P}^{i} \\ 1 \end{bmatrix} = \begin{bmatrix} \begin{pmatrix} \cos\theta_1^i \cos\theta_2^i \cos\theta_3^i \sin\theta_4^i L - \sin\theta_1^i \sin\theta_3^i \sin\theta_4^i L \\ -\cos\theta_1^i \sin\theta_2^i \cos\theta_4^i L - d^i \cos\theta_1^i \sin\theta_2^i + r_b \cos\theta_1^i \end{pmatrix} \\ \begin{pmatrix} \sin\theta_1^i \cos\theta_2^i \cos\theta_3^i \sin\theta_4^i L + \cos\theta_1^i \sin\theta_3^i \sin\theta_4^i L \\ -\sin\theta_1^i \sin\theta_2^i \cos\theta_4^i L - d^i \sin\theta_1^i \sin\theta_2^i + r_b \sin\theta_1^i \end{pmatrix} \\ \left(\sin\theta_2^i \cos\theta_3^i \sin\theta_4^i L + \cos\theta_2^i \cos\theta_4^i L + d^i \cos\theta_2^i\right) \\ 1 \end{bmatrix} \quad (1)$$

The corresponding homogeneous transformation of the moving platform can be written as [8]:

$${}^{B}_{M}\mathbf{T} = \begin{bmatrix} \mathbf{n} & \mathbf{o} & \mathbf{a} & {}^{B}_{M}\mathbf{P} \\ 0 & 0 & 0 & 1 \end{bmatrix} \quad (2)$$

The position vector of the moving platform with respect to the base frame is:

$${}^{B}_{M}\mathbf{P} = \frac{1}{3}\left({}^{B}_{5}\mathbf{P}^{1} + {}^{B}_{5}\mathbf{P}^{2} + {}^{B}_{5}\mathbf{P}^{3}\right) \quad (3)$$

The orientation of the moving platform with respect to the base frame is calculated from the position vector as:

$$\mathbf{n} = \frac{{}^{B}_{5}\mathbf{P}^{1} - {}^{B}_{M}\mathbf{P}}{\left|{}^{B}_{5}\mathbf{P}^{1} - {}^{B}_{M}\mathbf{P}\right|} \quad (4)$$

$$\mathbf{o} = \frac{{}^{B}_{5}\mathbf{P}^{2} - {}^{B}_{5}\mathbf{P}^{3}}{\left|{}^{B}_{5}\mathbf{P}^{2} - {}^{B}_{5}\mathbf{P}^{3}\right|} \quad (5)$$

$$\mathbf{a} = \mathbf{n} \times \mathbf{o} \quad (6)$$

3.2 *Forward kinematic of the slave manipulator*

The milling tool tip locations and orientations are found from a given set of joint variables $(l_1, l_2, l_3, l_4 \text{ and } \alpha)$ as shown in Figure 6. [7]

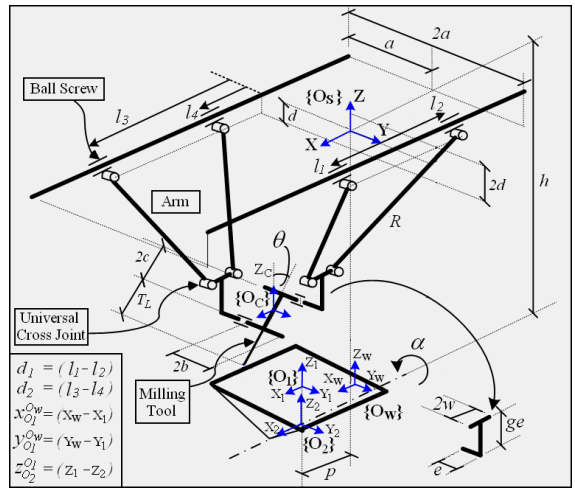

Figure 6: Manipulator joint's configuration

The rotating angles of the tool about Y axis can readily be determined as:

$$\cos\theta = \sqrt{1 - \left(\frac{l_1 + l_2 - l_3 - l_4}{4c}\right)^2} \quad (7)$$

The work piece coordinate {Ow} is related to the reference frame $\{O_S\}$. The milling tool tip locations on the work piece coordinate can be expressed by parameters that are corresponding to the reference frame as shown in equations (8-10):

$$x_w = \left(\frac{l_1 + l_2 + l_3 + l_4}{4}\right) - (c + T_L)\sin\theta - p + x_{o1}^{ow} \quad (8)$$

$$y_w = \left(z_c - (c + T_L)\cos\theta\right)\sin\alpha + h\sin\alpha + y_{o1}^{ow} + \left(\frac{d_1^2 - d_2^2 - 4w(d_1 - d_2) - 16(d - c\cos\theta)(z_c + ge)}{16(a - b - e)}\right)\cos\alpha \quad (9)$$

$$z_w = \left(z_c - (c + T_L)\cos\theta\right)\cos\alpha + h\cos\alpha + z_{O2}^{O1} - \left(\frac{d_1^2 - d_2^2 - 4w(d_1 - d_2) - 16(d - c\cos\theta)(z_c + ge)}{16(a - b - e)}\right)\sin\alpha \quad (10)$$

Where,

$$z_c = \frac{-W_2 \pm \sqrt{W_2^2 - 4W_1W_3}}{2W_1}$$

$$W_1 = \left(\frac{16^2 \left(d - c\cos\theta\right)^2}{128\left(a-b-e\right)^2} + 2 \right)$$

$$W_2 = \left(4ge + \frac{512ge(d - c\cos\theta)^2}{128\left(a-b-e\right)^2} - \frac{32(d - c\cos\theta)\left(d_1^2 - d_2^2 - 4w(d_1 - d_2)\right)}{128\left(a-b-e\right)^2} \right)$$

$$W_3 = \frac{16^2 (d - c\cos\theta)^2 ge^2}{128\left(a-b-e\right)^2} - \frac{32ge\ (d - c\cos\theta)\left(d_1^2 - d_2^2 - 4w(d_1 - d_2)\right)}{128\left(a-b-e\right)^2}$$
$$+ \frac{\left(d_1^2 - d_2^2 - 4w(d_1 - d_2)\right)^2}{128\left(a-b-e\right)^2} + \frac{\left(d_1^2 + d_2^2\right)}{4} + 2w^2 - w(d_1 + d_2) + 2ge^2$$
$$+ 2e^2 - 2R^2 + 2\left(b-a\right)^2 - 4e(a-b) + 2(c\cos\theta - d)^2$$

The direction cosine of work piece's cutting locations are defined from a rotating angle about Y axis (θ) and a rotating angle of the table (α) as shown in equations (11-13).

$$I_w = \pm \frac{1}{\sqrt{1 + \frac{1}{\tan^2\theta}}} \tag{11}$$

$$J_w = \pm \frac{1}{\left(\sqrt{1+\tan^2\theta}\right)\cdot\left(\sqrt{1+\tan^2(90-\alpha)}\right)} \tag{12}$$

$$K_w = \frac{\tan(90-\alpha)}{\left(\sqrt{1+\tan^2\theta}\right)\cdot\left(\sqrt{1+\tan^2(90-\alpha)}\right)} \tag{13}$$

Where,

$$sign(I_w) = sign(\theta)$$
$$sign(J_w) = sign(\alpha)$$
$$sign(K_w) = +$$

3.3 *Desired positions and orientations of the slave*

In case of difference joint configurations or dissimilar mechanisms, the master-slave manipulating tasks should be performed at Cartesian level as shown in Figure 7. The master arm's reference frame $\{O_M\}$ should have the same orientation as the slave reference frame $\{O_S\}$ for the sake of simplicity. Desired positions of the slave's milling tool $(\mathbf{X}_{sd})$ is achieved from the master arm's tip position $(\mathbf{X}_m)$ which is calculated from the master arm's forward kinematics, initial positions of the master arm $(\mathbf{X}_{mr})$, and initial position of the slave manipulator $(\mathbf{X}_{sr})$ as illustrated in equation (14).

G_P is applied for the master-slave scaling ratio which is normally equal to 1.

$$\mathbf{X}_{sd} = G_P \bullet (\mathbf{X}_m - \mathbf{X}_{mr}) + \mathbf{X}_{sr} \tag{14}$$

An orientation matrix of the slave's end-effector (milling tool) could not be considered directly from the master orientation matrix due to their dissimilar kinematics. To obtain the orientation matrix, we start with considering an orientation matrix of the master arm corresponding to its initial frame in equation (15-16).

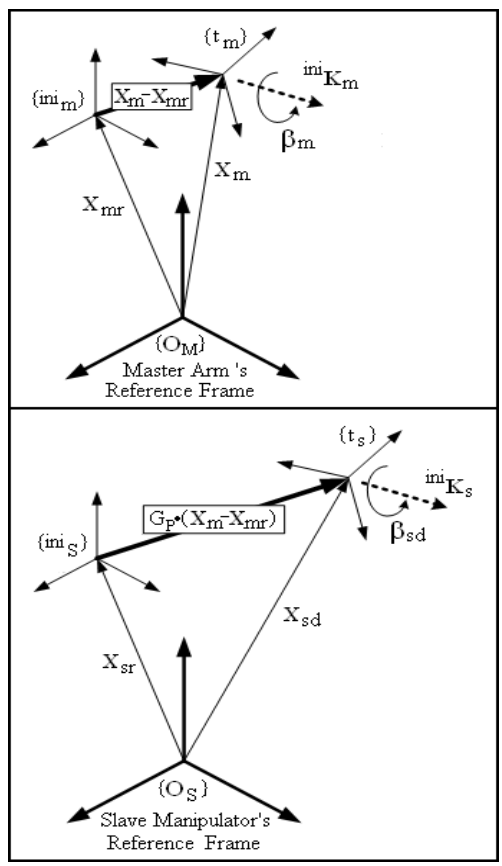

Figure 7: Desired positions and orientations of the slave manipulator

$$ {}^{ini}\mathbf{R}_m = \left({}^{0}\mathbf{R}_{mr} \right)^T \, {}^{0}\mathbf{R}_m \tag{15} $$

$$ {}^{ini}\mathbf{R}_m = \begin{bmatrix} rm_{11} & rm_{12} & rm_{13} \\ rm_{21} & rm_{22} & rm_{23} \\ rm_{31} & rm_{32} & rm_{33} \end{bmatrix} \tag{16} $$

The rotation about an arbitrary axis of the master arm in a Cartesian space, $\left({}^{ini}\mathbf{K}_m \right)$ and (β_m), is applied to define an arbitrary axis of the slave end-effector $\left({}^{ini}\mathbf{K}_s \right)$ and its rotating angle (β_{sd}) [10].

The master arm's rotating angle about an arbitrary axis is:

$$ \beta_m = \cos^{-1}\left(\frac{rm_{11} + rm_{22} + rm_{33} - 1}{2} \right) \tag{17} $$

An arbitrary axis of the master arm with respect to its initial coordinate is :

$$ {}^{ini}\mathbf{K}_m = \frac{1}{2\sin\beta_m} \begin{bmatrix} rm_{32} - rm_{23} \\ rm_{13} - rm_{31} \\ rm_{21} - rm_{12} \end{bmatrix} \tag{18} $$

We can find an arbitrary axis of the slave end-effector as follow:

$$ {}^{ini}\mathbf{K}_s = {}^{ini}_{0}\mathbf{R}_{sr} \, {}^{0}_{ini}\mathbf{R}_m \, {}^{ini}\mathbf{K}_m \tag{19} $$

In case of the same rotating angle as the master arm, the slave rotating angle is set equal to the master arm ($\beta_{sd} = \beta_m$).

The designed orientation matrix of the slave manipulator's tip referred to its base frame can be defined as equation (20), while its initial orientation matrix is ${}^{0}\mathbf{R}_{sr}$.

$$ {}^{0}\mathbf{R}_{sd} = {}^{0}\mathbf{R}_{sr} \, {}^{ini}\mathbf{R}_{sd} \tag{20} $$

Given,

$$ k_x = \frac{rm_{32} - rm_{23}}{2\sin\beta_m}, $$

$$ k_y = \frac{rm_{13} - rm_{31}}{2\sin\beta_m}, $$

$$ k_z = \frac{rm_{21} - rm_{12}}{2\sin\beta_m} $$

${}^{ini}\mathbf{R}_{sd}$ is defined as equation (21)

$$ {}^{ini}\mathbf{R}_{sd} = \begin{bmatrix} k_x k_x (1-\cos\beta_{sd}) + \cos\beta_{sd} & k_x k_y (1-\cos\beta_{sd}) - k_z \sin\beta_{sd} & k_x k_z (1-\cos\beta_{sd}) + k_y \sin\beta_{sd} \\ k_x k_y (1-\cos\beta_{sd}) + k_z \sin\beta_{sd} & k_y k_y (1-\cos\beta_{sd}) + \cos\beta_{sd} & k_y k_z (1-\cos\beta_{sd}) - k_x \sin\beta_{sd} \\ k_x k_z (1-\cos\beta_{sd}) - k_y \sin\beta_{sd} & k_y k_z (1-\cos\beta_{sd}) + k_x \sin\beta_{sd} & k_z k_z (1-\cos\beta_{sd}) + \cos\beta_{sd} \end{bmatrix} \tag{21} $$

3.4 *Geometrical Jacobian of the master arm*

Geometrical Jacobian is the relationship between the twist velocity of the moving platform and the velocity of the active joints that the actuators are attached. (There are some joints with no actuator attached). According to the relationship, $\mathbf{Bt} = \mathbf{A}\dot{\mathbf{q}}$, the matrices A and B are defined as matrices of the closed-loop chain [6].

$\mathbf{t}$ represents the velocity of the top plate which consists of the angular velocity (ω) and linear velocity (v).

$$ \mathbf{t} = \begin{bmatrix} \omega \\ v \end{bmatrix} = \begin{bmatrix} \omega_x & \omega_y & \omega_z & v_x & v_y & v_z \end{bmatrix}^T \tag{22} $$

$\dot{\mathbf{q}}$ represents the velocity of the joint variables where the actuators are attached.

$$ \dot{\mathbf{q}} = \begin{bmatrix} \dot{d}^1 & \dot{\theta}_3^1 & \dot{d}^2 & \dot{\theta}_3^2 & \dot{d}^3 & \dot{\theta}_3^3 \end{bmatrix}^T \tag{23} $$

According to Figure 8, the velocity of point $\mathbf{P}_j$ is:

$$ \dot{\mathbf{P}}_j = \dot{d}\mathbf{S}_{j1} + \dot{\theta}_3 \mathbf{S}_{j2} + \dot{\theta}_4 \mathbf{S}_{j3} \tag{24} $$

or

$$\dot{\mathbf{P}}_j = \mathbf{v} - \boldsymbol{\omega} \times \mathbf{r}_{mj} \tag{25}$$

Where,

$j = 1, 2, 3$

$$\mathbf{S}_{j1} = \mathbf{e}_j, \mathbf{S}_{j2} = \mathbf{f}_j \times \mathbf{r}_{fj}, \mathbf{S}_{j3} = \mathbf{g}_j \times \mathbf{r}_{gj},$$

$$\mathbf{r}_{mj} = \mathbf{P} - \mathbf{P}_j, \mathbf{r}_{fj} = \mathbf{r}_{gj} = \mathbf{P}_j - {}^{B}_{4}\mathbf{P}_j = \mathbf{P}_j - {}^{B}_{3}\mathbf{P}_j$$

$$\mathbf{r}_{fj} = L \begin{bmatrix} \left(\cos\theta_1 \cos\theta_2 \cos\theta_3 \sin\theta_4 - \sin\theta_1 \sin\theta_3 \sin\theta_4 \right) \\ \left(-\cos\theta_1 \sin\theta_2 \cos\theta_4 \right) \\ \left(\sin\theta_1 \cos\theta_2 \cos\theta_3 \sin\theta_4 + \cos\theta_1 \sin\theta_3 \sin\theta_4 \right) \\ \left(-\sin\theta_1 \sin\theta_2 \cos\theta_4 \right) \\ \left(\sin\theta_2 \cos\theta_3 \sin\theta_4 + \cos\theta_2 \cos\theta_4 \right) \end{bmatrix}_j$$

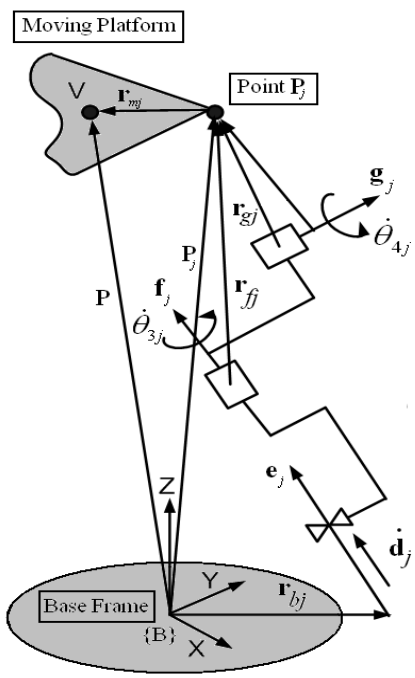

Figure 8: The position vector of link j

In order to find the geometrical Jacobian matrix, A and B would be formed first as shown below:

$$\mathbf{A} = \begin{bmatrix} a_{11} & 0 & 0 & 0 & 0 & 0 \\ 0 & a_{12} & 0 & 0 & 0 & 0 \\ 0 & 0 & a_{21} & 0 & 0 & 0 \\ 0 & 0 & 0 & a_{22} & 0 & 0 \\ 0 & 0 & 0 & 0 & a_{31} & 0 \\ 0 & 0 & 0 & 0 & 0 & a_{32} \end{bmatrix} \tag{26}$$

$$\mathbf{B} = \begin{bmatrix} \left(\mathbf{I}_1 \times \mathbf{r}_{m1}\right)^T & \mathbf{I}_1^T \\ \left(\mathbf{M}_1 \times \mathbf{r}_{m1}\right)^T & \mathbf{M}_1^T \\ \left(\mathbf{I}_2 \times \mathbf{r}_{m2}\right)^T & \mathbf{I}_2^T \\ \left(\mathbf{M}_2 \times \mathbf{r}_{m2}\right)^T & \mathbf{M}_2^T \\ \left(\mathbf{I}_3 \times \mathbf{r}_{m3}\right)^T & \mathbf{I}_3^T \\ \left(\mathbf{M}_3 \times \mathbf{r}_{m3}\right)^T & \mathbf{M}_3^T \end{bmatrix} \tag{27}$$

Where,

$j = 1,\ 2,\ 3$

$$a_{j1} = -\cos\theta_{j4}$$

$$a_{j2} = -\sin\theta_{j4} L$$

The unit vector parallel to vector $\left(\mathbf{S}_{j2} \times \mathbf{S}_{j3}\right)$ is :

$$\mathbf{I}_j = \frac{\mathbf{S}_{j2} \times \mathbf{S}_{j3}}{\left|\mathbf{S}_{j2} \times \mathbf{S}_{j3}\right|} \tag{28}$$

$$\mathbf{I}_j = \begin{bmatrix} \left(\sin\theta_1 \sin\theta_3 \sin\theta_4 - \cos\theta_1 \cos\theta_2 \cos\theta_3 \sin\theta_4 \right) \\ \left(+\cos\theta_1 \sin\theta_2 \cos\theta_4 \right) \\ \left(-\cos\theta_1 \sin\theta_3 \sin\theta_4 - \sin\theta_1 \cos\theta_2 \cos\theta_3 \sin\theta_4 \right) \\ \left(+\sin\theta_1 \sin\theta_2 \cos\theta_4 \right) \\ \left(-\sin\theta_2 \cos\theta_3 \sin\theta_4 - \cos\theta_2 \cos\theta_4 \right) \end{bmatrix}_j \tag{29}$$

The unit vector parallel to vector $\left(\mathbf{S}_{j3} \times \mathbf{S}_{j1}\right)$ is :

$$\mathbf{M}_j = \frac{\mathbf{S}_{j3} \times \mathbf{S}_{j1}}{\left|\mathbf{S}_{j3} \times \mathbf{S}_{j1}\right|} \tag{30}$$

$$\mathbf{M}_j = \begin{bmatrix} \left(\cos\theta_1 \cos\theta_2 \sin\theta_3 + \sin\theta_1 \cos\theta_3 \right) \\ \left(\sin\theta_1 \cos\theta_2 \sin\theta_3 - \cos\theta_1 \cos\theta_3 \right) \\ \left(\sin\theta_2 \sin\theta_3 \right) \end{bmatrix}_j \tag{31}$$

The Jacobian matrix can be formed as:

$$\mathbf{J} = \mathbf{A}^{-1}\mathbf{B} \tag{32}$$

The relationship between generated force at the handle of the master arm and applied torques of the attached DC motors can be written as:

$$\mathbf{F} = \mathbf{J}^{T}\boldsymbol{\tau} \tag{33}$$

Where,

$\mathbf{F} = \begin{bmatrix} M_x & M_y & M_z & F_x & F_y & F_z \end{bmatrix}^T$ is the vector of moment (M) and force (F) generating against the operator hand on the master arm's handle.

$\boldsymbol{\tau} = \begin{bmatrix} f_1 & \tau_1 & f_2 & \tau_2 & f_3 & \tau_3 \end{bmatrix}^T$ consists of forces and torques of the master arm's motors where $f_i \left(i = 1,2,3\right)$ are applied forces at prismatic joints (d^i) and $\tau_i \left(i = 1,2,3\right)$ are applied torques at revolute joints $\left(\theta_3^i\right)$.

4 Experimental Results

To indicate the master-slave positions in a 3D workspace by measuring data from the attached encoders, the master arm's handle tip is performed to move inside its workspace. In this way, the slave manipulator's tip is controlled through the desired positions and orientations that are calculated from section 3.3. The master arm's tip positions and the slave manipulator's tip positions are illustrated from the starting point to the finishing point in view of the slave's work piece coordinate as shown in Figure 9.

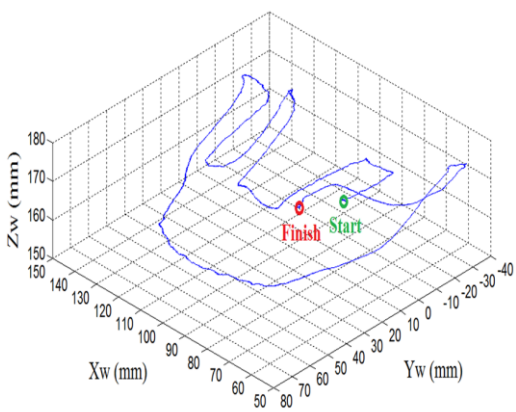

Figure 9: Master-Slave tip positions in 3D workspace of the slave manipulator (work piece coordinate) on each sampling time

With respect to the starting point, the master arm's tip positions on each sampling times in Xw, Yw and Zw direction of the work piece coordinate are shown in Figure 10. The operator changes his hand movement in Yw direction more than others as indicated by its magnitude of the positions. The maximum position error is appeared in Yw direction as shown in Figure 11. The slave manipulator can follow the master tip's position on each sampling time with a position error of less than 1.0 mm. However, the position error considered in this work is calculated from the attached encoders that can be used to indicate the master-slave operating system but wouldn't guarantee the structural errors generated from misalignment of the mechanisms.

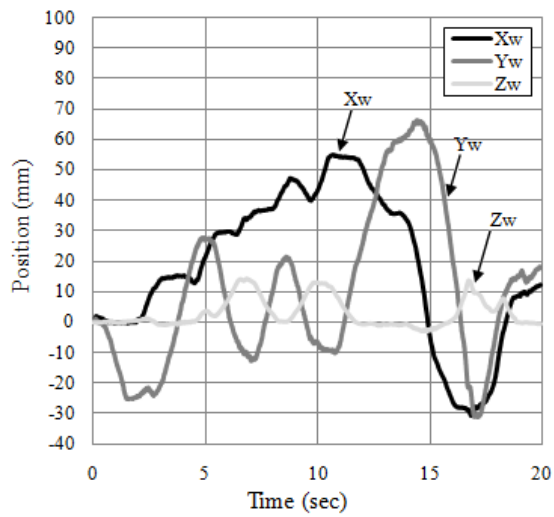

Figure 10: Positions of the slave manipulator's tip compared to the starting point in work piece coordinate

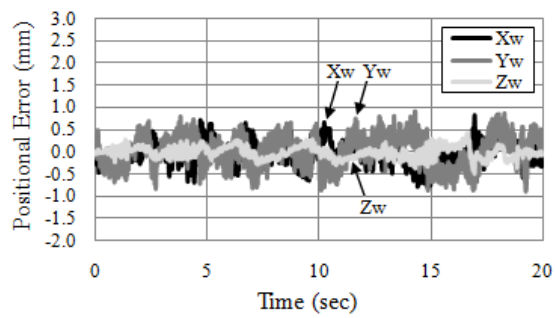

Figure 11: Position error between the master arm's tip and the slave manipulator's tip in work piece coordinate

The rotating angles of the slave manipulator's tip about Y axis (θ) and the rotating angles of the table about X axis (α) which are referred to the starting values are shown in Figure 12. This rotation is manipulated by the operator through the master arm's handle tip when the master-slave system is operated in a 3D workspace. Rotating angles are dependent on the operator's hand orientation. Rotational deviations from the reference data are shown in Figure 13. In this experiment, rotational deviations are less than 0.5 degrees calculated from the measured data of attached encoders. However, the rotation about Z axis of the master arm is diminished in the slave manipulator site due to its less degree of freedom.

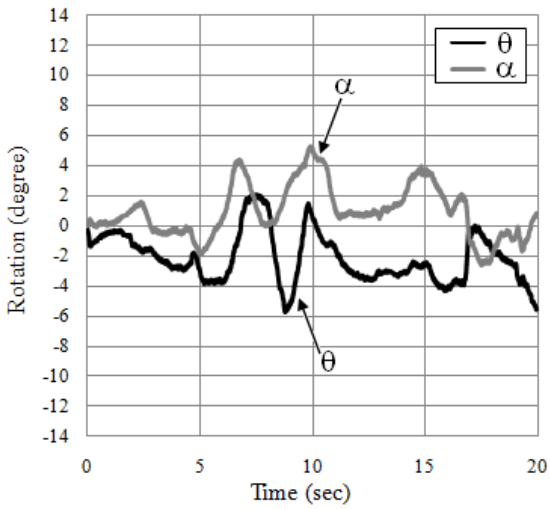

Figure 12: Rotating angles about Y axis of the slave manipulator's tip and rotating angles of the table compared to the starting point

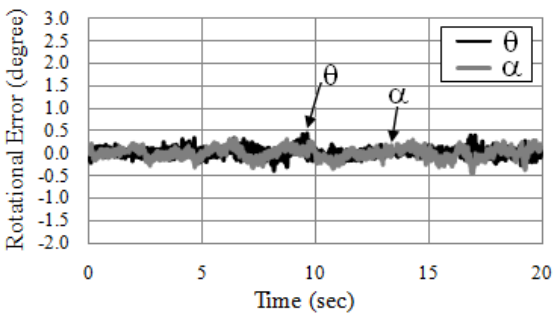

Figure 13: Rotation error between the master arm's tip and the slave manipulator's tip

To study the force reflection against the operator hand, a virtual wall is applied on the master arm's reference frame to restrict the movement of master arm's handle in -X direction as shown in Figure 14. The virtual wall position is moved along -X axis causing the available working area for the master arm's handle tip to be on the referenced object. The operator will feel the reflected force from his hand while the handle tip is moved inside the virtual wall area. The reflection force is generated from DC motors that are attached to the actuated joints of the master arm. The relationship between the force reflection and the required DC motor torques is mentioned in section 3.4.

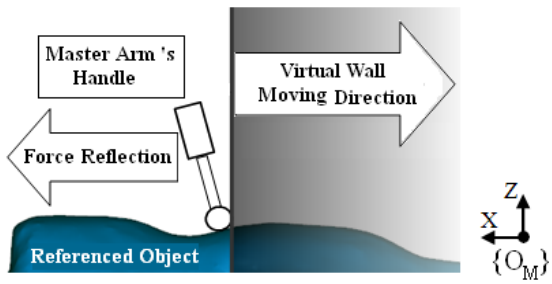

Figure 14: Virtual wall moving direction used in the force reflection test.

In Figure 15, the master arm's tip is moved interacting with a virtual wall that is located parallel to YZ plane of the master arm reference frame at X equal to -20 mm. During the movement, the master arm's tip positions are distorted from the referenced value of the virtual wall (X= -20mm).

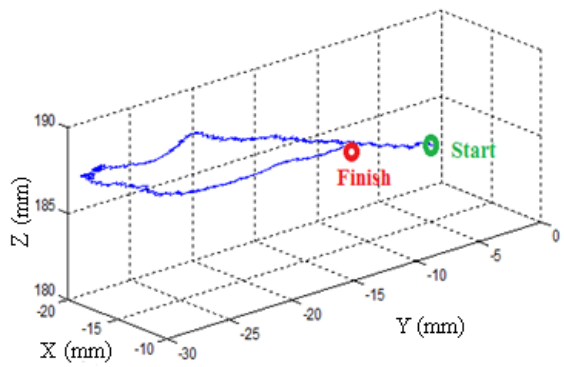

Figure 15: The master arm's tip positions on the virtual wall plane.

In Figure 16, the master arm's tip position usually appeared inside the virtual wall area when the virtual wall is located at X equal to -20 mm. In this way, the master arm will generate force reflection against the operator's hand related to its deviations in X direction as shown in Figure 17. The force reflection is performed in the opposite direction of position error between the master arm and referenced virtual wall location. However, the force reflection against the operator's hand is set to zero when the master arm's tip is brought out of the virtual wall area.

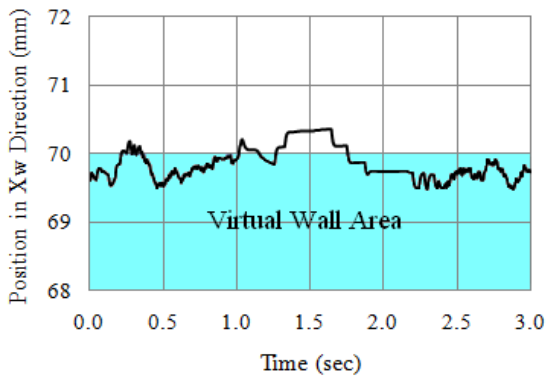

Figure 16: The master arm's tip positions in X direction and virtual wall area

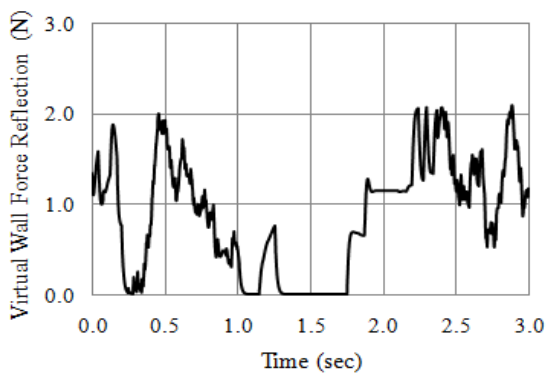

Figure 17: Force reflection against the operator's hand in X direction

To demonstrate the force reflection occurring from the master-slave in the slot milling task, the master arm is performed to move in Y direction only. In Figure 18, the master arm's tip position which is used as reference Yw in work piece coordinate is compared to the measured data of the slave manipulator. The slave manipulator's tip can follow the master arm's tip position at each sampling time with a position error of approximately less than 0.8 mm. In this case, the master arm will generate force reflection against the operator's hand in the opposite direction of the positional error as shown in Figure 19. The force reflection in this work is 2.5 times of the position error. With a feeling of significant force reflection, the operator will adapt his/her hand movement to change the cutting feed rate of the milling tool which is located at the slave manipulator side.

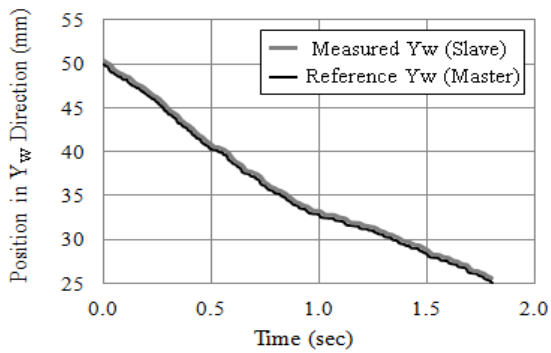

Figure 18: Referenced Yw of the master arm's tip position and measured Yw of the slave manipulator

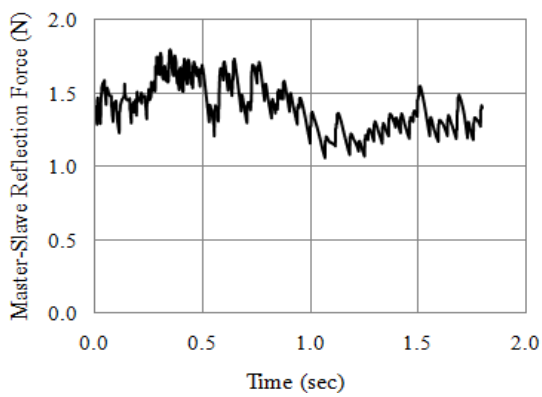

Figure 19: Force reflection in Y direction generated from master-slave position error in Yw direction

In order to start the material removal process, the operator installs the referenced object on the master arm's base frame and puts a raw or stock material at the rotating table on the slave arm side. The operator moves the handle tip, which is made from 3.5 mm. steel ball along the surface of the referenced object. In this way, the end-effecter of the slave manipulator which is installed with a 6.0 mm diameter-ball-end milling tool will remove material from the stock simultaneously. According to different diameters between the master arm's steel ball and the slave's milling tool, the experimental results must be considered with compensated dimensions.

The concave-bottle shape referenced object and its reproduced wooden work piece is shown in Figure20. The compensated dimensions of the referenced object should be 83.8 mm. in height and 28.1 mm. in width. However, the work piece produced by the slave manipulator has approximately 1.2 mm. height error and 0.6 mm. width error (width error 0.3 mm on each side).

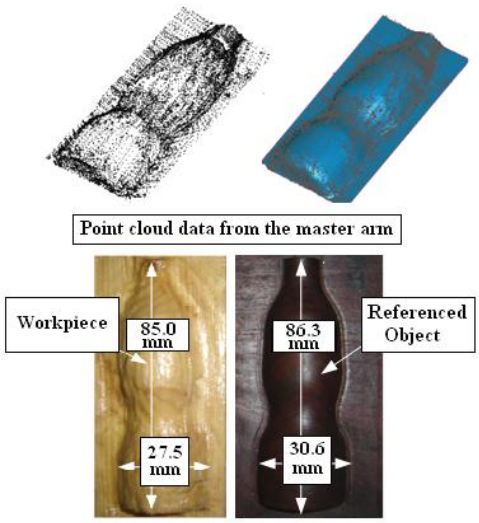

Figure 20: Dimensions of the concave-bottle shape referenced object and the work piece created by the master-slave system

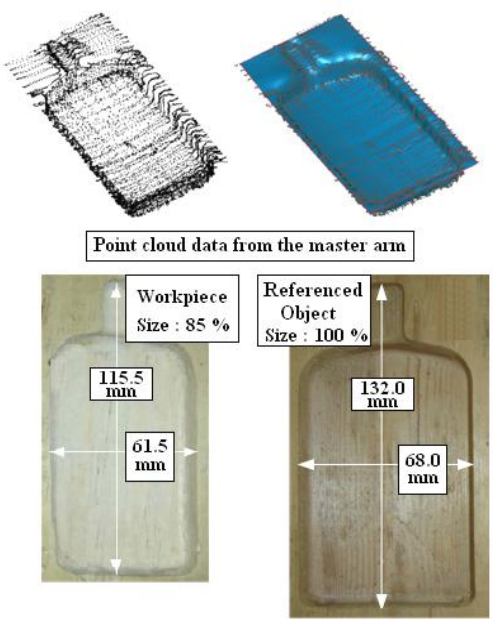

Figure 21: Dimensions of the convex-bottle shape referenced object and the work piece created by the master-slave system (Reduce size to 85%)

The comparison between the convex bottle shape referenced object and its reproduced wooden work piece is shown in Figure 21. In this case, we mention on scaling the work piece dimensions to 85% of the referenced object. Thus, the scaling factor (G_P), which is indicated in equation (14), must be equal to 0.85. The compensated dimensions of the referenced object should be 114.3 in height and 59.9 in width. However, the work piece produced by the slave manipulator has approximately 1.2 mm height error and 1.6 mm. width error (width error 0.8 mm on each side).

5 Conclusions

This paper presented a master-slave operating technique which is aimed to be used for a man-machine material removal process. The experimental results show that the slave manipulator's tip position can follow the master arm's tip position moving by the operator's hand in a 3D workspace. The virtual wall force reflection in X direction is varied according to the deviation between the master arm's tip and the virtual wall. The master-slave force reflection is applied to the master arm side for the feeling of force against the operator hand while the milling tool removes the material from the stock. Two work pieces produced from this technique have similar shapes compared with their referenced objects. The dimension error on each side of the work pieces is approximately less than 1.0 mm.

Acknowledgements

This work is sponsored by Chulalongkorn University under Chulalongkorn University Centenary Academic Development Project.

References

[1] Zhengji Teng, Hsi-Yung Feng and Abdullahil Azeem. 2006. *Generating efficient tool paths from point cloud data via machining area segmentation*, International Journal of Advance Manufacturing Technology Vol.30. 2006, pp. 254-260.

[2] K.L. Chui, W.K. Chui and K.M. Yu. 2008. *Direct 5-axis tool-path generation from point cloud input using 3D biarc fitting*, Robotics and Computer-Integrated Manufacturing Vol.24. 2008, pp. 270-286.

[3] Erdem Ozturk, L.Taner Tunc, Erhan Budak, 2009. Investigation of lead and tilt angle effects in 5-axis ball-end milling processes, International Journal of Machine Tools & Manufacture Vol.49 2009, pp. 1053-1062.

[4] Ismail Lazoglu. 2003. *Sculpture surface machining : a generalized model of ball-end milling force system*, International Journal of Machine Tools & Manufacture Vol.43 2003, pp. 453-462.

[5] Asier Ibeas and Manuel de la Sen. 2006. *Robustly Stable Adaptive Control of a Tandem of Master-Slave Robotic Manipulators With Force Reflection by Using a Multiestimation Scheme*, IEEE Transactions on Systems, MAN, and Cybernetics Vol.36. 2006, pp. 1162-1179.

[6] Viboon Sangveraphunsiri, Tawee Ngamvilaikorn 2005. *Design and Analysis of a 6-DOF Haptic Device for Teleoperation Using a Singularity - Free Parallel Mechanism*, Thammasasat International Journal of Science and Technology Vol.14.2005. pp. 60-69.

[7] Viboon Sangveraphunsiri, Kummun Chooprasird. 2011. *Dynamics and Control of a 5-DOF Manipulator Base on an H-4 Parallel Mechanism*, International Journal of Advance Manufacturing Technology Vol.52. 2011, pp. 343-364.

[8] Pawel Malysz and Shahin Sirouspour. 2009. *Nonlinear and Filtered Force/Position Mappings in Bilateral Teleoperation With Application to Enhanced Stiffness Discrimination*, IEEE Transactions on Robotics Vol.25. 2009, pp. 1134-1149.

[9] Sanjit Moshat, Saurav Datta, Asish Bandyopad-hyay and Pradip Kumar Pal. 2010. *Optimization of CNC end milling process parameters using PCA-based Taguchi method* , International Journal of Engineering, Science and Technology Vol.2 No.1 2010, pp 92-102.

[10] Sciavicco L. and Siciliano B. 1996. *Modeling and control of robot manipulators*, MacGraw-Hill, New York.